JOURNAL OF GUIDANCE, CONTROL, AND DYNAMICS
Vol. 30, No. 3, May–June 2007

Feedback-Based Steering Law for Control Moment Gyros

Alexandre N. Pechev*
Surrey Space Centre, University of Surrey, Guildford, GU2 7XH England, United Kingdom

DOI: 10.2514/1.27351

A new approach for solving the singularity avoidance problem is presented, based on the observation that the gimbal rates can be derived by minimizing (in a feedback loop) the difference between the demanded torque and the control moment gyro output torque. The derivations are approached from a control prospective, but the final solution results in a structure very similar to the classical singularity robust steering law. Some differences, however, need to be acknowledged. Because the gimbal rates are related to the demanded torque through the control sensitivity function, the solutions are generated in a feedback loop, and thus the algorithm does not require computations of matrix inversion and matrix determinant. The steering law has a dynamic structure, and a relationship is established between the torque error and the gimbal-rate capacity of the actuator. The new steering law also breaks the symmetry in the computation in the gimbal rates, and thus the gimbal trajectories avoid the internal singularities, rather than passing through them. Consequently, the full control moment gyro momentum space is used. Examples with some typical maneuvers are presented to justify this numerically. For the derivation of the steering law, $\mathcal{H}_\infty$ theory is used, and an efficient adaptation algorithm is developed to account for the dependence of the Jacobian on the gimbal angles. Derivation and implementation steps are presented with numerical examples.

I. Introduction

A ROTOR spinning at a constant speed can be gimbaled to produce a gyroscopic torque on the spacecraft. The control moment gyro (CMG) is an attitude control actuator that works on this principle. The direction of the angular momentum is determined by one or more motorized gimbal mechanisms. The output torque is proportional to the rate of change of the momentum and is controlled through the gimbal rate. Because the gyroscopic torque is considerably larger than the input gimbal torque, the CMG is power efficient [1,2]. Better pointing accuracy can be also expected by selecting rotor speeds that avoid excitations of resonance modes in the chassis. In the past, CMGs have been used mainly on large spacecraft platforms such as the Mir Space Station and the International Space Station. Recently, the need for agile small satellites with high pointing accuracy has created a renewed interest in this actuator [3,4]. The number of controlled gimbals classifies the CMG as a single-gimbal or a double-gimbal actuator. This paper considers only the single-gimbal CMG.

One of the difficulties associated with CMGs is the existence of singular states at which the actuators fail to deliver the required torque about a specific demanded direction. This is equivalent to aligning the torque outputs from the individual CMGs on a plane with the demanded torque direction being normal to this plane. From a practical prospective, avoiding singularities requires redundant configurations with the number of CMGs higher than the number of controlled degrees of freedom. *Steering laws* are used in conjunction with the attitude controller to avoid or transit through the singularities. A detailed characterization and classification of the singularities in a cluster of CMGs was developed by Margulies and Aubrun [1]. Since then, a considerable amount of effort has been made in the area of designing steering laws and attitude control loops with CMGs. These are categorized here as error-free singularity avoidance laws and pseudo-inverse-based avoidance laws. In the former type, global search methods have been proposed to find optimal gimbal-angle trajectories for a given demanded torque profile, such that the singular states are avoided [5]. Although this is an optimal solution, this feedforward approach is of limited use for feedback applications. For a redundant CMG configuration, a local gradient search can be used to derive gimbal rates in the locality of the singular state, such that the gimbal motions do not produce torque [6]. These null-motion-based techniques, however, do not guarantee global singularity avoidance.

The second class of singularity avoidance laws is based on different forms of the pseudo-inverse method. A common characteristic for these methods is the approximation in the solution for the gimbal rates near the singularity, resulting in a finite torque error. The minimum two-norm Moore–Penrose pseudo-inverse method is the simplest, but symmetry in the computation of the gimbal rates forces the CMG cluster to a singular state. This, in turn, leads to excessively large gimbal rates. A solution to this is the singularity robust (SR) steering law proposed by Bedrossian [7], which was adapted from inverse kinematic solutions for robot manipulators. In the vicinity of the singularity, the SR law generates feasible solutions for the gimbal rates at the expense of some error between the demanded torque and the output torque. The shortcoming of the SR law is that if trapped in a special class of singular states, the algorithm fails to deliver solutions [6,8]. To overcome this limitation, several approaches have been proposed. Oh and Vadali [9] present an adaptation scheme in which the SR law is kept unchanged, but the demanded torque is perturbed in the vicinity of the singularity by introducing off-diagonal terms in the attitude controller. Wie and coworkers [8] developed the generalized singularity robust steering law, which uses time-dependent modulation functions in the calculation of the gimbal rates. This law was later modified to handle a special class of saturation singularities [10]. Ford and Hall [11] make use of the singular avoidance parameter to improve on the tracking of the demanded torque. Other methods have been proposed that combine robust inverse and null motion, for example [6]. Important developments are also presented in [12–14].

In this paper, the singularity avoidance problem is approached from a control point of view. The steering algorithm is derived based on the observation that the gimbal rates can be computed by minimizing (in a feedback loop) the difference between the demanded torque and the CMG output torque. It is demonstrated that the gimbal rates are related to the demanded torque through the control sensitivity function, and in structure, the latter closely resembles the classical singularity robust steering law. Furthermore, because the gimbal rates are computed in a feedback loop, the algorithm does not require computations of matrix inversion and matrix determinant. A relationship is also established between the

Received 17 August 2006; revision received 29 November 2006; accepted for publication 29 November 2006.

*a.pechev@surrey.ac.uk.

torque error and the gimbal-rate capacity of the actuator. The new steering law also breaks the symmetry in the computation of the gimbal rates, and as a result, the gimbal trajectories avoid internal singularities, leading to high values for the CMG momentum, in comparison with SR-based approaches. The involvement of the feedback control machinery to the problem of steering CMGs opens up new opportunities for assessing the robustness of steering laws.

The subsequent part of the paper is organized as follows. First, a brief review is given to some of the pseudo-inverse-based steering laws. The feedback-based steering law is then introduced, and discussions on the stability and the performance are included in Sec. III.A, with some parallels drawn between the new steering law and the classical inversion-based approaches. Because this law depends on the derivation of a control function, an adaptive $\mathcal{H}_\infty$-based control algorithm is developed. Numerical examples, discussions on the real-time implementation, and a set of simulation results are presented.

II. Pseudo-Inverse-Based Steering Laws for CMGs

A single-gimbal CMG is depicted in Fig. 1a, in which α represents the *gimbal* angle in respect to an actuator-fixed reference frame and $\mathbf{h}$ is the angular momentum vector. The CMG output torque is controlled by commanding the rate of change of the momentum vector. In a typical attitude control system, three or more CMGs are arranged to provide full three-axis control. The total momentum vector is a sum of the individual momentum vectors $\mathbf{h}_i$ ($i = 1, \cdots, N$ where N is the number of CMGs). A commonly studied CMG redundant configuration is the pyramid arrangement presented in Fig. 1b. Because the overall momentum vector is a nonlinear function of the gimbal angles, the output torque is also a nonlinear function of the gimbal angles through the Jacobian $\mathbf{J}(\alpha)$ as follows:

$$\dot{\mathbf{h}} = \frac{\partial \mathbf{h}(\alpha)}{\partial t} = \frac{\mathrm{d}\mathbf{h}}{\mathrm{d}\alpha}\frac{\mathrm{d}\alpha}{\mathrm{d}t} = \mathbf{J}(\alpha)\dot{\alpha} \tag{1}$$

In the general case, $\alpha = [\alpha_1, \alpha_2, \cdots, \alpha_N]^T$ and $\mathbf{J}(\alpha) \in \mathbb{R}^{3\times N}$. For Fig. 1b, $N = 4$, $\beta = 54.74$ deg, and

$$\mathbf{J}(\alpha) = \begin{bmatrix} -c_\beta \cos\alpha_1 & \sin\alpha_2 & c_\beta \cos\alpha_3 & -\sin\alpha_4 \\ -\sin\alpha_1 & -c_\beta \cos\alpha_2 & \sin\alpha_3 & c_\beta \cos\alpha_4 \\ s_\beta \cos\alpha_1 & s_\beta \cos\alpha_2 & s_\beta \cos\alpha_3 & s_\beta \cos\alpha_4 \end{bmatrix} \tag{2}$$

where c_β and s_β are constants corresponding to $\cos(\beta)$ and $\sin(\beta)$, respectively. We refer to the representation in Eq. (1) as the CMG model. This model is a simplification of the real CMG dynamics, because the control input is taken to be the gimbal velocity $\dot{\alpha}$ and the inertia of the individual gimbals are excluded from the representation. To simplify the analysis, most of the steering laws presented in the literature resort to this assumption. Contrary to all other design methods, however, the approach developed in this paper

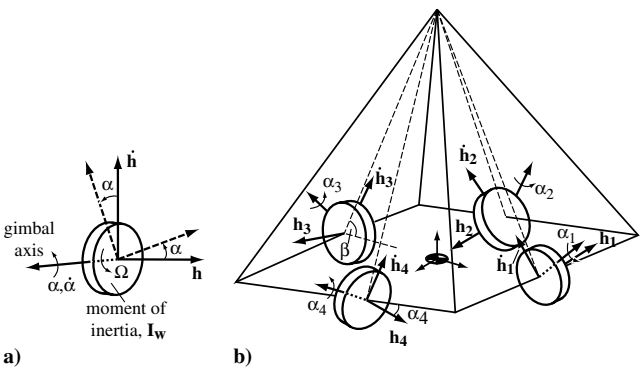

Fig. 1 Graphical representation of a) the control moment gyroscope (the gimbal axis is controlled by a motorized mechanism with a permissible gimbal rate $\dot{\alpha}$; for $\dot{\alpha} = \alpha = 0$, the momentum of the wheel is $\mathbf{h} = \mathbf{h_0} = \mathbf{I_w\Omega}$) and b) a cluster of four CMGs mounted on a pyramid with a skew angle of $\beta = 54.74$ deg.

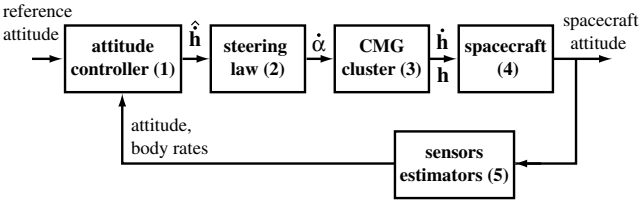

Fig. 2 CMG-based attitude control system.

provides the necessary machinery for incorporating the dynamics of the individual gimbals into the steering law design.

A typical CMG-based attitude control system is shown in Fig. 2. The attitude control law (block 2) produces the demanded CMG torque $\hat{\mathbf{h}}$. The steering law, in turn, delivers the required gimbal rates for given $\hat{\mathbf{h}}$. With the assumption that three CMGs are used for three-axis attitude control, a simple steering law reduces to solving Eq. (1) for $\dot{\alpha}$:

$$\dot{\alpha} = \mathbf{J}^\dagger(\alpha)\hat{\mathbf{h}} \tag{3}$$

where $\mathbf{J}^\dagger(\alpha)$ represents the inverse of $\mathbf{J}(\alpha)$. The practical difficulty of this approach is the existence of gimbal combinations (or singular states [1]) for which $\mathbf{J}(\alpha) \in \mathbb{R}^{3\times 3}$ loses rank. Because in a singular configuration all row elements of $\mathbf{J}(\alpha)$ become zero, the corresponding torque output vanishes regardless of the applied rates $\dot{\alpha}$. Redundant configurations with a number of CMGs higher than the number of controlled axes are thus a preferred option, because the additional degrees of freedom allow finding alternative solutions. For the arrangement in Fig. 1b, the minimum norm solution to the following problem

$$\min_{\dot{\alpha}} \|\dot{\alpha}\|^2, \quad \text{subject to } \dot{\mathbf{h}} = \mathbf{J}(\alpha)\dot{\alpha} \tag{4}$$

gives the Moore–Penrose inverse

$$\mathbf{J}^\dagger(\alpha) = \mathbf{J}(\alpha)^T[\mathbf{J}(\alpha)\mathbf{J}(\alpha)^T]^{-1} \tag{5}$$

This algorithm, however, also fails when the rank of $\mathbf{J}(\alpha)$ is less than three. In the vicinity of the singular point, $\det[\mathbf{J}(\alpha)\mathbf{J}(\alpha)^T]$ approaches zero, resulting in excessively large solutions for $\dot{\alpha}$. To overcome this problem, the singularity robust steering law is proposed [7] as a solution to the following minimization problem ($\mathbf{K_1} > 0$ and $\mathbf{K_2} > 0$):

$$\min_{\dot{\alpha}} \frac{1}{2}\begin{bmatrix} \dot{\mathbf{h}} - \mathbf{J}(\alpha)\dot{\alpha} \\ \dot{\alpha} \end{bmatrix}^T \begin{bmatrix} \mathbf{K_1} & 0 \\ 0 & \mathbf{K_2} \end{bmatrix} \begin{bmatrix} \dot{\mathbf{h}} - \mathbf{J}(\alpha)\dot{\alpha} \\ \dot{\alpha} \end{bmatrix} \tag{6}$$

The unique optimal solution for $\dot{\alpha}$ results in the singularity robust inverse [for readability, α is dropped from the notation of $\mathbf{J}(\alpha)$]:

$$\mathbf{J}^\dagger = \mathbf{J^T K_1}\left(\mathbf{JJ^T K_1} + \mathbf{K_2}\right)^{-1} \tag{7}$$

Although any positively definite gain matrices $\mathbf{K_1}$ and $\mathbf{K_2}$ will satisfy the solution, in the SR steering law, these are set to [6] $\mathbf{K_1} = \mathbf{I}$ and $\mathbf{K_2} = \lambda\mathbf{I}$, resulting in

$$\mathbf{J}^\dagger = \mathbf{J}^T(\mathbf{JJ}^T + \lambda\mathbf{I})^{-1} \tag{8}$$

The emphasis here is that this particular combination for $\mathbf{K_1}$ and $\mathbf{K_2}$ provides only one feasible solution, and in the following section, this statement is clarified. In the preceding representation, λ is a scalar that expresses the tradeoff between exactness and feasibility of the solution [6]. In the vicinity of the singular state, λ is modified to guarantee the solvability of the matrix inverse [9]:

$$\lambda = \lambda_0 \exp[-\mu \det(\mathbf{JJ}^T)] \tag{9}$$

where λ_0 and μ are positive constants. The solution for the gimbal rates using the SR law then becomes

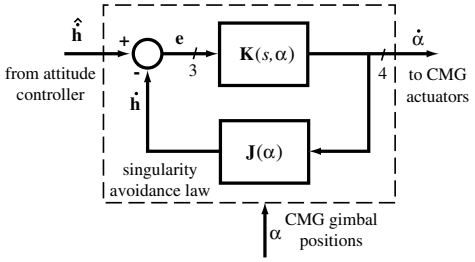

Fig. 3 Feedback singularity avoidance control law.

$$\dot{\alpha} = \mathbf{J}^T(\mathbf{J}\mathbf{J}^T + \lambda\mathbf{I})^{-1}\hat{\dot{\mathbf{h}}} \tag{10}$$

Although the SR law is computationally efficient, the algorithm still fails to deliver a solution if the system does become singular due to the imperfection in the knowledge of $\mathbf{J}$ [8]. The steering law in Eq. (10) will therefore not be able to escape from the singular state. Oh and Vadali [9] propose to keep the steering law unchanged but to perturb the demanded torque $\hat{\dot{\mathbf{h}}}$ instead in the vicinity of the singularity by modifying the attitude control law (block 1 in Fig. 2). An important step forward has been made by Wie et al. [8] by proposing $\mathbf{K_2}$ to be extended to a full matrix with the off-diagonal terms being harmonic time-dependent functions, for example,

$$\dot{\alpha} = \mathbf{J}^T(\mathbf{J}\mathbf{J}^T + \lambda\mathbf{E})^{-1}\hat{\dot{\mathbf{h}}} \tag{11}$$

where

$$\mathbf{E} = \begin{bmatrix} 1 & \epsilon_0\sin(\varpi t + \phi_1) & \epsilon_0\sin(\varpi t + \phi_2) \\ \epsilon_0\sin(\varpi t + \phi_1) & 1 & \epsilon_0\sin(\varpi t + \phi_3) \\ \epsilon_0\sin(\varpi t + \phi_2) & \epsilon_0\sin(\varpi t + \phi_3) & 1 \end{bmatrix} \tag{12}$$

This generalized singularity robust law requires setting $\epsilon_0, \phi_1, \phi_2, \phi_3$, and ϖ, in addition to λ_0 and μ [8,10,15]. The design of the new feedback singularity (FS) law is discussed next. In the process of the derivation, some parallels with the preceding steering laws are made.

III. Feedback Singularity Avoidance Control Law

The FS law proposed in this paper uses control theory for the solution to the steering problem. The idea is depicted in Fig. 3. The design goal is the minimization of the difference between the demanded torque $\hat{\dot{\mathbf{h}}}$ and the CMG output torque $\dot{\mathbf{h}}$ in a feedback configuration. For the purpose of the analysis, we first make the assumption that $\mathbf{K}(s)$ is known. Figure 3 then suggests that the gimbal rates are related to the commanded torque through the control sensitivity function:

$$\dot{\alpha} = \mathbf{K}(s)[\mathbf{J}\mathbf{K}(s) + \mathbf{I}]^{-1}\hat{\dot{\mathbf{h}}} \tag{13}$$

Turning our attention now to the developments in Sec. II, it is interesting to note that the FS law is very similar in structure to the SR law in Eq. (10). The latter statement requires setting λ to 1 and replacing $\mathbf{J}^T$ with $\mathbf{K}(s)$. Because the SR law was derived from the minimization of Eq. (6), the particular choice of $\mathbf{K_1} = \mathbf{I}$ and $\mathbf{K_2} = \lambda\mathbf{I}$ represents only a single possible solution. The argument here is that any positive definite $\mathbf{K_1}$ and $\mathbf{K_2}$ in Eq. (7) will render a stable solution, but the particular choice has an impact on the performance. This has been somewhat justified through the developments in [8] and the modifications in Eq. (11). Equation (13) also shows that the inversion is performed indirectly through the feedback loop, and the implementation of the steering law reduces to a filter (more details are given in Sec. IV.A). Note that the steering law in Eq. (13) can be also equivalently represented as $\dot{\alpha} = [\mathbf{K}(s)\mathbf{J} + \mathbf{I}]^{-1}\mathbf{K}(s)\hat{\dot{\mathbf{h}}}$.

To correlate the output torque with the demanded torque, the complementary function is derived

$$\dot{\mathbf{h}} = \mathbf{J}\mathbf{K}(s)[\mathbf{J}\mathbf{K}(s) + \mathbf{I}]^{-1}\hat{\dot{\mathbf{h}}} \tag{14}$$

To achieve the required identity between the demanded torque and the output torque (i.e., $\dot{\mathbf{h}} \equiv \hat{\dot{\mathbf{h}}}$) $\mathbf{K}(s)$, needs to be designed such that it delivers at steady state

$$\mathbf{T} = \mathbf{J}\mathbf{K}(s)[\mathbf{J}\mathbf{K}(s) + \mathbf{I}]^{-1} = \mathbf{I} \tag{15}$$

In this respect, a key element in the proposed new method is the compensator $\mathbf{K}(s)$.

For the design of $\mathbf{K}(s)$, the following constraints need to be imposed. First, because the Jacobian $\mathbf{J}(\alpha)$ depends on the gimbal angles α, the controller has to be adapted by taking information for α. Second, singularity phenomena have to be taken into account. To satisfy this requirement, $\mathbf{K}(s)$ needs to be a full transfer matrix to provide a solution even when $\mathbf{J}(\alpha)$ loses rank at a particular singular direction. It is interesting to note that this is quite opposite to the choice of $\mathbf{K_1} = \mathbf{I}$, proposed for the SR law in Eq. (6) [the same observation has been made when deriving the generalized steering law in Eq. (11), but the author's choice is to instead *modulate* the identity matrix]. In the vicinity of the singular point, the nonzero components of the torque error $\mathbf{e} = \hat{\dot{\mathbf{h}}} - \dot{\mathbf{h}}$ would generate finite values for the gimbal rates through the off-diagonal elements of $\mathbf{K}(s)$. This will steer the CMGs away from the singularity for the expense of some perturbations on the attitude. In Sec. III.A, we also demonstrate that only a system that is capable of delivering indefinitely large gimbal rates can steer through a singularity without an error. This conclusion can be also made directly from Eq. (5), but for the FS law design, this is connected with the practical constraints in the actuator. The development in the following section allows drawing relationships between the admissible torque error and the gimbal-rate capacity in the system, and this has not been previously addressed in a formal way in the design of steering laws. The SR-based approaches deal with it through different gain factors such as λ, μ, etc.

A. Main Result

To connect the new steering law to the pseudo-inverse-based approaches, we first present the main result of this paper. Following the design process developed in Sec. IV, the optimal adaptive feedback law $\mathbf{K}(s)$ that solves the feedback-based steering problem in Fig. 3 has the following form

$$\mathbf{K}(s) = \mathbf{J}^T\mathcal{Q} \tag{16}$$

where

$$\mathcal{Q} = \mathcal{P}(s\mathbf{I} - \mathcal{A}_\mathcal{K})^{-1}\mathcal{B}_\mathcal{K} \tag{17}$$

$\mathcal{P} \in \mathbb{R}^{3\times3}$ is a positive definite symmetric gain matrix, $\mathcal{A}_\mathcal{K} \in \mathbb{R}^{3\times3}$ is a negative definite diagonal matrix, and $\mathcal{B}_\mathcal{K} \in \mathbb{R}^{3\times3}$ is a positive definite diagonal matrix. The specific numerical values are related to the bandwidth of the steering law and the upper bound on the gimbal rates. Substituting Eq. (16) into Eq. (13) transforms the FS law into

$$\dot{\alpha} = \mathbf{J}^T\mathcal{Q}(\mathbf{J}\mathbf{J}^T\mathcal{Q} + \mathbf{I})^{-1}\hat{\dot{\mathbf{h}}} \tag{18}$$

Several conclusions can be drawn from this. To first prove the internal stability for the FS law, one has to guarantee that

$$\det(\mathbf{J}\mathbf{J}^T\mathcal{Q} + \mathbf{I}) \neq 0 \tag{19}$$

It can be shown that this is same as ensuring that the singular values

$$\sigma(\mathbf{J}\mathbf{J}^T\mathcal{Q}) \geq 0 \tag{20}$$

for all combinations in the gimbal angles. For $\mathcal{Q} = \mathcal{Q}^T \geq 0$, this requirement is always satisfied.

Another interesting property of the new algorithm is that the SR law in Eq. (10) can be transformed to a feedback steering law by setting $\lambda = 1$ and $\mathbf{K_1} = \mathcal{Q}$. In fact, in a very special case, s can be set

to 0 to consider only the steady-state control matrix

$$\bar{\mathcal{Q}} = \mathcal{P}(-\mathcal{A}_{\mathcal{K}})^{-1}\mathcal{B}_{\mathcal{K}} \tag{21}$$

and to rewrite the steering law in Eq. (18) using $\bar{\mathcal{Q}}$

$$\dot{\alpha} = \mathbf{J}^T\bar{\mathcal{Q}}(\mathbf{J}\mathbf{J}^T\bar{\mathcal{Q}} + \mathbf{I})^{-1}\hat{\dot{\mathbf{h}}} \tag{22}$$

It is useful to note that Eq. (22) provides both singularity avoidance and singularity escaping properties, similar to the generalized singularity law in Eq. (11). In addition, because $\bar{\mathcal{Q}}$ is a full transfer matrix, the solutions for the gimbal rates are nonsymmetric, resulting in singularity avoidance properties. Although $\bar{\mathcal{Q}}$ can be any positive definite transfer matrix, the particular numerical form connected to the system's constraints and the required performance are of benefit.

B. Torque Error

Finally, the torque error in the loop needs discussion. The output torque is related to the demanded torque via the complementary sensitivity function:

$$\dot{\mathbf{h}} = \mathbf{J}\mathbf{J}^T\mathcal{Q}(\mathbf{J}\mathbf{J}^T\mathcal{Q} + \mathbf{I})^{-1}\hat{\dot{\mathbf{h}}} \tag{23}$$

The torque error, on another hand, is related to the demanded torque through the sensitivity function:

$$\mathbf{e} = (\mathbf{J}\mathbf{J}^T\mathcal{Q} + \mathbf{I})^{-1}\hat{\dot{\mathbf{h}}} \tag{24}$$

The preceding equation suggests that there will be always some error between the demanded torque and the output torque. It is important to note that this is also true for all singularity robust-based laws, because the product of the singular values of $\mathbf{J}\mathbf{J}^T$ is always finite, resulting in nonzero values for λ in Eqs. (10) and (11). For the FS law, however, the error is proportional to the size of $\mathcal{Q}$. Furthermore, in the following section, it is shown that $\mathcal{Q}$ is proportional to the square of the maximum gimbal rate that the actuators can achieve. Therefore, only a system that is capable of achieving indefinitely large gimbal rates can pass through the singularity without perturbations. The fact that the practical limits of the actuator can be connected with the error in the steering law is an advantage, because it provides an input for the hardware design when the pointing requirements are predefined.

Considering the dynamics of the compensator, it is interesting to note that the size of $\mathcal{Q}$ depends on the complex frequency. Also, this size can be increased at steady state if $\mathcal{A}_{\mathcal{K}}$ in Eq. (17) is set to zero. This transforms the feedback compensator to a transfer matrix constructed of pure integrators. Therefore, at steady state ($s \approx 0$) $\mathbf{J}\mathbf{J}^T\mathcal{Q} \gg \mathbf{I}$ results in vanishingly small torque error. From a practical prospective, however, some upper limits on the gain of $\mathbf{K}(s)$ at low frequency are expected, providing a nonzero $\mathcal{A}_{\mathcal{K}}$. The derivation of $\mathbf{K}(s)$ in Eq. (16) is presented next.

IV. Controller Derivation

For the derivation of $\mathbf{K}(s)$, a two-step approach is proposed. The controller is first designed with the assumption that $\mathbf{J}$ is constant. An adaptation loop is then derived that modifies $\mathbf{K}(s)$ to account for the dependence of the Jacobian on the gimbal angles.

A. $\mathcal{H}_\infty$ Design

For the design of $\mathbf{K}(s)$, $\mathcal{H}_\infty$ control theory is employed [16]. The optimization goal is to minimize, in an ∞-norm sense, the mapping from the demanded torque to the torque error $\mathbf{e} = \hat{\dot{\mathbf{h}}} - \dot{\mathbf{h}}$. From a practical prospective, the gimbal rates are also constrained. This requires setting the following optimization problem:

$$\min_{\mathbf{K}(s)} \left\| \begin{pmatrix} \mathbf{w_1}(s)[\mathbf{I} + \mathbf{J}\mathbf{K}(s)]^{-1} \\ \mathbf{w_2}\mathbf{K}(s)[\mathbf{I} + \mathbf{J}\mathbf{K}(s)]^{-1} \end{pmatrix} \right\|_\infty \tag{25}$$

In the preceding penalty, two weighting functions are included. The weighting function $\mathbf{w_1}(s)$ bounds the sensitivity function and essentially determines the bandwidth of the steering law. A finite value for the bandwidth is justifiable, because the CMG model is a part of the feedback and finite acceleration rates are expected. In comparison, the SR-based approaches assume infinitely large bandwidth. The weighting function $\mathbf{w_2}$ puts an upper bound on the gimbal rates $\dot{\alpha}$. As discussed in the previous section, this has a direct impact on the torque error.

For the derivation of the controller, the generalized plant is constructed [16]. First, we define the performance weights

$$\mathbf{w_1}(s) := \begin{bmatrix} \mathbf{A} & \mathbf{B} \\ \mathbf{C} & \mathbf{0} \end{bmatrix}, \qquad \mathbf{w_2} := \frac{1}{w}\mathbf{I}^{4\times 4} \tag{26}$$

To simplify the presentation, we assume that all CMGs have the same upper limit on the gimbal rate w. With this assumption, the generalized open-loop model becomes

$$\dot{x} = \mathbf{A}x + \mathbf{B}\hat{\dot{\mathbf{h}}} - \mathbf{B}\mathbf{J}\dot{\alpha} \qquad \mathbf{z} = \begin{bmatrix} \mathbf{0} \\ \mathbf{C} \end{bmatrix}x + \begin{bmatrix} \mathbf{w_2} \\ \mathbf{0} \end{bmatrix}\dot{\alpha}$$
$$\mathbf{e} = \mathbf{I}\hat{\dot{\mathbf{h}}} - \mathbf{J}\dot{\alpha} \tag{27}$$

where $\mathbf{z}$ represents a penalty variable, and the controller's task is to minimize the size of the mapping from $\hat{\dot{\mathbf{h}}}$ to $\mathbf{z}$ [16]. For a full transfer form of $\mathbf{K}(s)$, nonzero gimbal angles are chosen to get $\mathbf{J} = \mathbf{J}(\alpha_0)$, where $\alpha_0 \neq 0$. For the design of $\mathbf{K}(s)$, the optimization task in Eq. (25) can be solved by a standard $\mathcal{H}_\infty$ controller-optimization algorithm [16]. A numerical example is given in Sec. IV.A.

For the adaptation of $\mathbf{K}(s)$, an efficient method that guarantees the stability in Eq. (14) is necessary. We start our analysis by representing the controller in an observer-based form:

$$\mathbf{K}(s): \begin{matrix} \dot{\hat{x}} = \mathcal{A}_{\mathcal{K}}\hat{\mathbf{x}} + \mathcal{B}_{\mathcal{K}}\mathbf{e} \\ \dot{\alpha} = \mathcal{C}_{\mathcal{K}}\hat{\mathbf{x}} \end{matrix} \tag{28}$$

The state-feedback part of the controller can be rewritten as

$$\mathcal{C}_{\mathcal{K}} = \mathbf{J}^T b w^2 \bar{\mathcal{P}} \tag{29}$$

where $\bar{\mathcal{P}} > 0$, $\bar{\mathcal{P}} = \bar{\mathcal{P}}^T$ is the solution of the Riccati equation associated with the state-feedback design [16]. Equation (29) suggests that the controller in the steering law can be directly adapted by updating $\mathcal{C}_{\mathcal{K}}$ using the current gimbal angles α and, hence, $\mathbf{J}$. As a result, the form in Eq. (18) is derived. For the representation in Eq. (29), we assume that all three directions for the torque are weighted equally. Setting $\mathbf{w_1}(s)$ to be a first-order weighting function, the transfer matrices reduce to $\mathbf{B} = b\mathbf{I}^{3\times 3}$ and $\mathbf{C} = \mathbf{I}^{3\times 3}$, where b is the required bandwidth in the steering law. Based on the preceding, some interesting conclusions can be made. As identified earlier, the torque error is proportional to the size of $\mathcal{P} = bw^2\bar{\mathcal{P}}$:

$$\mathcal{Q} = bw^2\bar{\mathcal{P}}(s\mathbf{I} - \mathcal{A}_{\mathcal{K}})^{-1}\mathcal{B}_{\mathcal{K}} \tag{30}$$

Consequently, the torque error is proportional to the square of the maximum gimbal rate the actuators can achieve times the bandwidth frequency b. We stress that $\mathcal{B}_{\mathcal{K}}$ and $\bar{\mathcal{P}}$ are also functions of b; therefore, the impact of b on the size of the torque error is not as easy to distinguish as the effect of w^2. This completes the design of the singularity avoidance control law. A numerical example is presented in the following section.

B. Numerical Example

The performance weights are specified to start the numerical design. The bandwidth of the FS law (Fig. 3) is fixed at 30 rad/s. All three torque components are weighted equally, resulting in a common pole in $\mathbf{w}_1(s)$. At low frequency, the sensitivity is limited to below -50 dB. The upper bound on the gimbal rates is fixed at 1.8 rad/s for all four gimbals. This results in

$$[\mathbf{w_1}(s)]^{-1} = \frac{30}{s+0.05}\begin{bmatrix}1&0&0\\0&1&0\\0&0&1\end{bmatrix}, \qquad \mathbf{w_2} = \frac{1}{1.8}\begin{bmatrix}1&0&0&0\\0&1&0&0\\0&0&1&0\\0&0&0&1\end{bmatrix} \tag{31}$$

For the linearization of the Jacobian in Eq. (2), we select $\alpha_0 = [\pi, \pi/4, -\pi/4, \pi]$, resulting in $\beta = 54.74^0$:

$$\mathbf{J}(\alpha_0) = \begin{bmatrix} 0.6000 & 0.7071 & 0.4243 & 0.0000 \\ 0.0000 & -0.4243 & -0.7071 & -0.6000 \\ -0.8000 & 0.5657 & 0.5657 & -0.8000 \end{bmatrix} \tag{32}$$

With these inputs, the $\mathcal{H}_\infty$ controller using a standard state-space approach is designed. The numerical form of the individual matrices in the solution [Eq. (28)] are given next:

$$\begin{bmatrix}\mathcal{A}_\mathcal{K} & \mathcal{B}_\mathcal{K}\\ \mathcal{C}_\mathcal{K} & 0\end{bmatrix} = \left[\begin{array}{cccccc} -0.05 & 0 & 0 & 2.18 & 0 & 0 \\ 0 & -0.05 & 0 & 0 & 2.18 & 0 \\ 0 & 0 & -0.05 & 0 & 0 & 2.18 \\ 49.72 & 34.15 & -17.05 & & & \\ 31.83 & 7.71 & 10.09 & & \mathbf{0} & \\ -7.71 & -31.83 & 10.09 & & & \\ -34.15 & -49.72 & -17.05 & & & \end{array}\right] \tag{33}$$

The controller has three state variables contributed from the pole of $\mathbf{w_1}(s)$. It is evident that due to the values in $\mathcal{A}_\mathcal{K}$, $\mathbf{K}(s)$ behaves almost as an integrator. The solution to the Riccati equation for the feedback part gives the following positive definite matrix

$$\bar{\mathcal{P}} = \begin{bmatrix} 11.51 & 8.31 & -0.18 \\ 8.31 & 11.51 & 0.18 \\ -0.18 & 0.18 & 2.89 \end{bmatrix} \tag{34}$$

By employing this in Eq. (29), the adaptive form of the control law is derived:

$$\mathcal{C}_\mathcal{K}(\alpha) = \mathbf{J}(\alpha)^T(1.8^2)(2.18)\bar{\mathcal{P}} \tag{35}$$

$\mathcal{C}_\mathcal{K}$ is adapted at every sample by calculating $\mathbf{J}(\alpha)$ in Eq. (2).

V. Simulations

In this section, the FS law in Eq. (13) is compared numerically with the generalized SR steering law in Eq. (11) [8]. The simulation parameters are listed in Table 1. The rotational motion of the spacecraft with a cluster of CMGs is described as

$$\mathcal{I}\,\dot{\omega} + \omega \times (\mathcal{I}\omega + \mathbf{h}) = -\dot{\mathbf{h}} + \mathbf{T_e} \tag{36}$$

where ω is a vector of body angular rates, $\mathbf{h}$ is the CMG total momentum vector in body coordinates, $\mathcal{I}$ is the principal moment of inertia of the spacecraft, and $\mathbf{T}_e$ is the external torque. The gimbal dynamics are excluded from the rotational motion. To describe the attitude, we use the quaternion kinematic dynamic equation:

Table 1 Simulation and design parameters

Parameter	Value	Units
$\mathbf{h_0}$	0.2795	Nms
$\mathbf{k_1}$	$1.5 \times \mathbf{I}^{(3\times3)}$	
$\mathbf{k_2}$	$6.0 \times \mathbf{I}^{(3\times3)}$	
$\mathcal{I}$	$10 \times \mathbf{I}^{(3\times3)}$	$\mathrm{kg}\cdot\mathrm{m}^2$
ω_0	$[0,0,0]^T$	rad/s
$[\lambda_0, \mu, \epsilon_0]$	[0.01,10,0.01]	
$[\varpi, \phi_1, \phi_2, \phi_3]$	$[0.5, 0, \pi/2, \pi]$	

$$\dot{\mathbf{q}} = \tfrac{1}{2}\mathbf{G}(\mathbf{q})\omega, \qquad \mathbf{G}(\mathbf{q}) = \begin{bmatrix} -q_1 & -q_2 & -q_3 \\ q_0 & -q_3 & q_2 \\ q_3 & q_0 & -q_1 \\ -q_2 & q_1 & q_0 \end{bmatrix} \tag{37}$$

Because the derivation of the attitude control law (block 1 in Fig. 2) is not the primary objective of this study, a simple state-feedback control law is used for all simulations, which provides the Lyapunov stable closed-loop attitude system with inputs from the quaternion error $\mathbf{q_e}$ and the spacecraft angular rates ω:

$$\hat{\dot{\mathbf{h}}} = \mathbf{k_1}\mathbf{q_e} + \mathbf{k_2}\omega \tag{38}$$

Perfect measurements are assumed for both attitude position and body rates.

The singularity avoidance properties of the FS law are analyzed. For this, a step change demand of 40 degrees on the x axis is requested, to force the CMG cluster through an elliptic internal singularity [8,10]. A selection of responses using the SR steering law in Eq. (11) is presented in Figs. 4 and 5 (left-hand side). A common characteristic of all SR-based steering laws is the symmetry in the generation of the gimbal rates (Fig. 4a). This, in turn, forces the CMGs toward the elliptic internal singularity. At $t \approx 4$ s, the gimbals settle to $[-\pi/2, 0, \pi/2, 0]$, with coplanar torque outputs from two CMG actuators and zero torque outputs from the other two. The Jacobian matrix becomes singular, leading to a zero value for the singularity index in Fig. 4g. The CMG momentum is saturated to

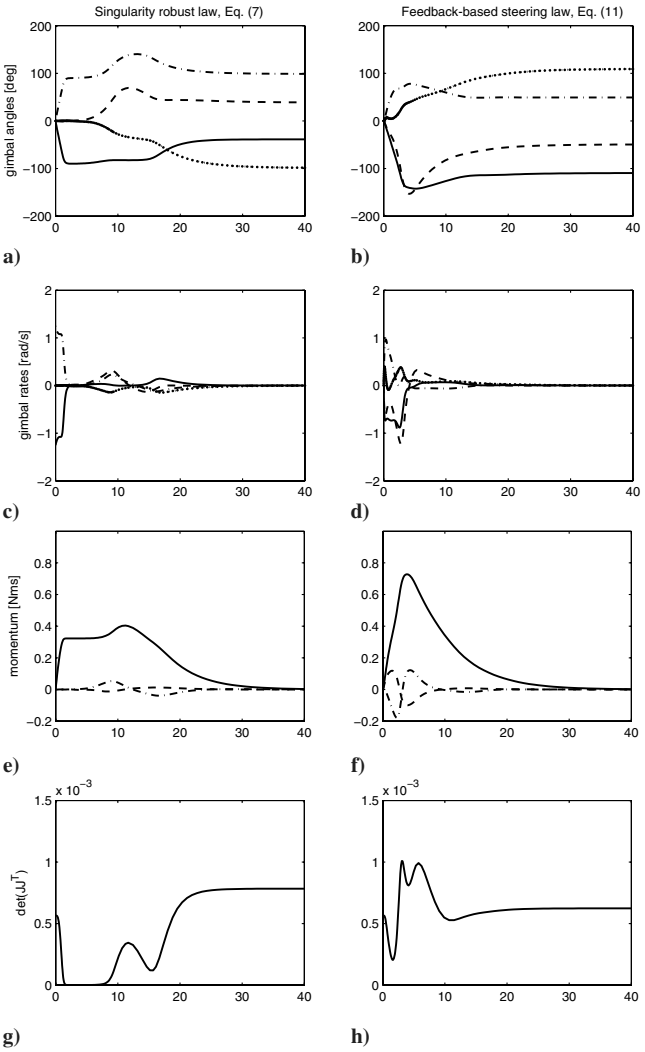

Fig. 4 Responses for a 40-deg roll maneuver starting from $\alpha = [0, 0, 0, 0]^T$; generalized singularity robust steering law [Eq. (11)] (left), and feedback-based steering law [Eq. (13)] (right).

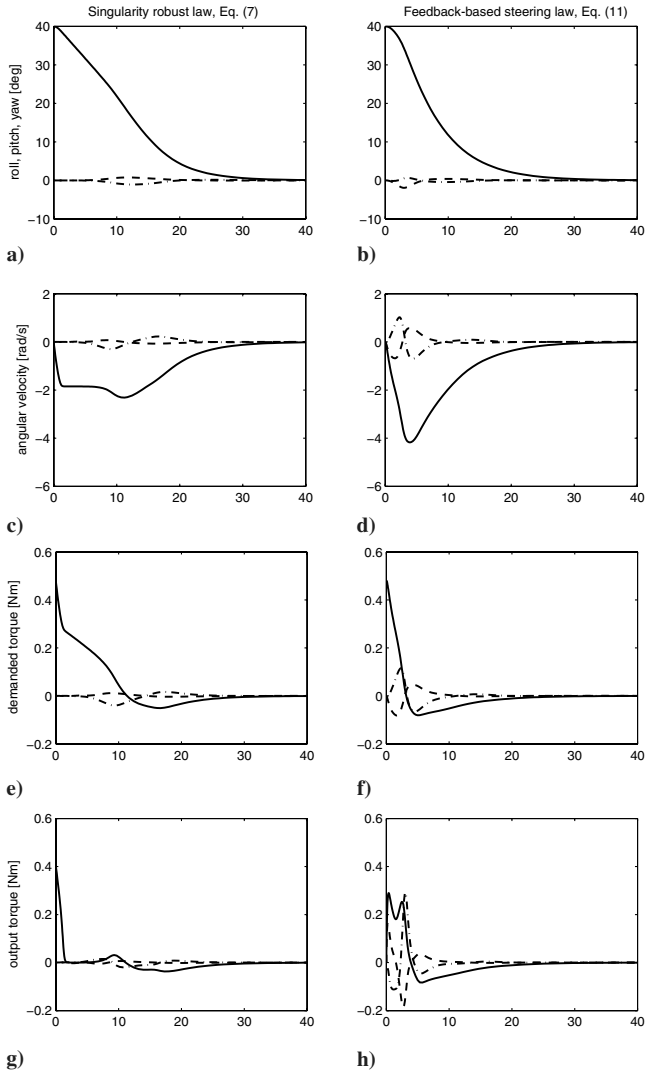

Fig. 5 Responses for a 40-deg roll maneuver starting from $\alpha = [0, 0, 0, 0]^T$; generalized singularity robust steering law [Eq. (11)] (left), and feedback-based steering law [Eq. (13)] (right).

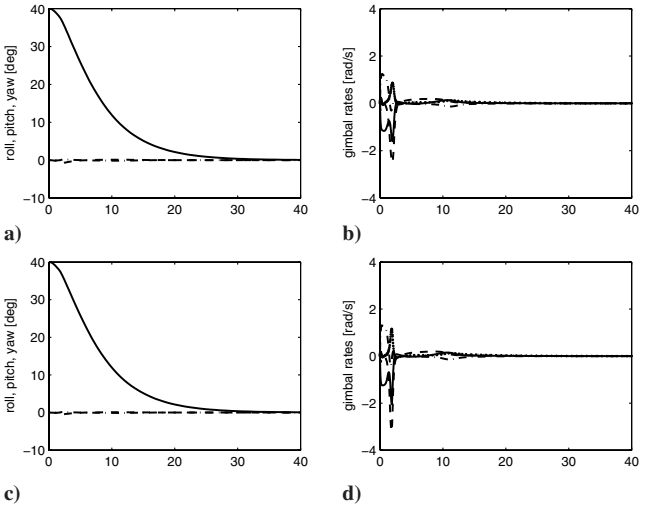

Fig. 6 Effects of gimbal-rate capacity on the attitude error: a) $w = 3$ rad/s, b) $w = 3$ rad/s, c) $w = 4$ rad/s, and d) $w = 4$ rad/s.

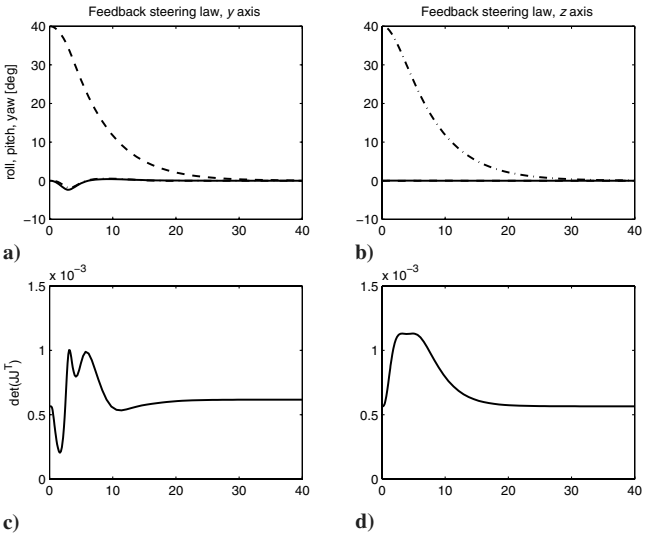

Fig. 7 FS steering law; $w = 1.8$ rad/s; 40-deg y-axis maneuver (left) and 40-deg z-axis maneuver (right).

approximately one-third of its maximum (Fig. 4e), leading to a saturation in the spacecraft's body rates ω (Fig. 5c). Because the gimbal rates are also close to zero at this saturation point ($2 \le t \le 6$ s), the attitude feedback loop is essentially ineffective (Fig. 5a).

For the same reference demand, the response from the FS law is presented in Figs. 4 and 5 (right-hand side). It is evident from the responses (Fig. 4b) that this law breaks the symmetry in the generation of the gimbal angles. This is mainly contributed to the form of $\mathcal{Q}$ in Eq. (18). As a result, the response does not pass intentionally through the singularity, and thus the singularity index, Fig. 4h, is always larger than zero [here, the response of $\det(\mathbf{J}\mathbf{J}^T)$ is used only for the purpose of the comparison]. Because the FS law does not force the CMGs through the singularity, higher magnitudes for the total CMG momentum are achieved for the same reference demand (Fig. 4f), leading to faster transient response (Fig. 5b). A comparison between the demanded torque $\hat{\dot{\mathbf{h}}}$ and the CMG output torque $\dot{\mathbf{h}}$ is shown in Figs. 5e–5h. The peak for this maneuver is below 0.4 Nm for both algorithms. The peak on the attitude error is around 1 deg (Figs. 5a and 5b). By design (Sec. IV.A), the gimbal rates are constrained to below 1.8 rad/s, and the results show that this is satisfied (Fig. 4d). Because the FS law does not depend on the distance from a singular point, the error in the response is somewhat distributed, rather than concentrated near singular gimbal configurations. A previous argument was that the algorithms will always lead to some torque error, due to the limitations in the actuator. Provided that the gimbal mechanisms are capable of delivering higher values for the gimbal rates, the FS law can be redesigned. Two such examples are included: Figs. 6a and 6b for $w = 3$ rad/s and Figs. 6c and 6d for $w = 4$ rad/s, respectively. In comparison with the results in Figs. 4b and 5b, these new values lead to a larger size for $\mathcal{Q}$, and hence the torque error is reduced to below 0.1 deg with $\|\dot{\alpha}\|_\infty < 3$ rad/s.

Considering other maneuvers, we demonstrate that the FS law is also capable of handling pitch and yaw demands without any redesign and modifications; responses are presented in Fig. 7. The maximum gimbal rate for all CMGs is set to 1.8 rad/s. The singularity index is included to demonstrate the effectiveness of keeping the gimbal trajectories away from singular points.

In the final round of simulations, the singularity escaping properties are studied. For this, the initial gimbal angles are set to $\alpha = [-\pi/2, 0, \pi/2, 0]$, with corresponding responses shown in Figs. 8 and 9. Similar to the SR steering law, the feedback-based law escapes the internal singularity and successfully escapes from the saturation singularity at $t \approx 8$ s.

VI. Conclusions

In this paper, a new method for steering control moment gyroscopes is presented, based on the observation that the gimbal rates can be derived by minimizing (in a feedback loop) the

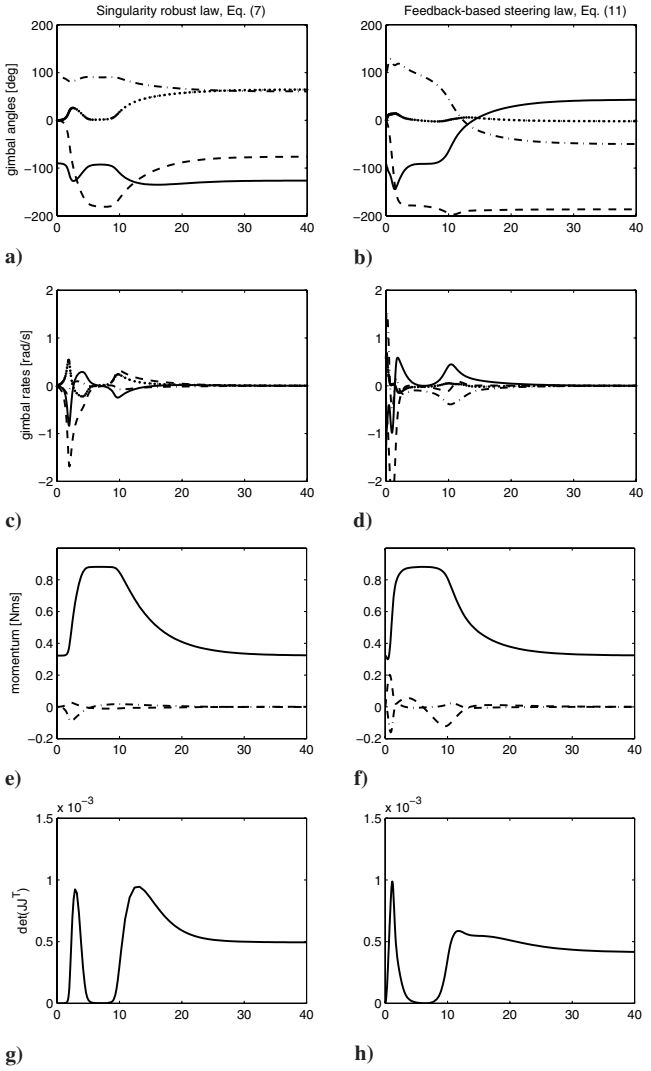

Fig. 8 Responses for a 40-deg roll maneuver starting from an elliptic singularity with $\alpha = [-\pi/2, 0, \pi/2, 0]$; generalized singularity robust steering law [Eq. (11)] (left), and feedback-based steering law [Eq. (13)] (right).

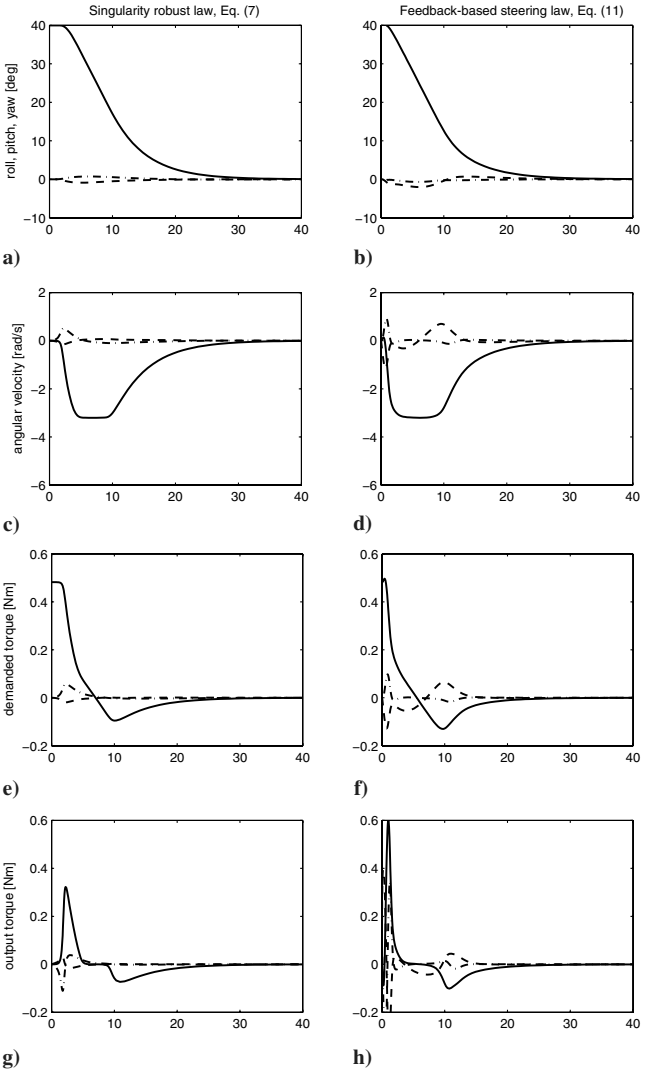

Fig. 9 Responses for a 40-deg roll maneuver starting from an elliptic singularity with $\alpha = [-\pi/2, 0, \pi/2, 0]$; generalized singularity robust steering law [Eq. (11)] (left), and feedback-based steering law [Eq. (13)] (right).

difference between the demanded torque and the CMG output torque. The derivations are approached from a control prospective and it is demonstrated that the gimbal rates and the demanded torque are related through the control sensitivity function. Because the solutions are generated in a feedback loop, the algorithm does not require computations of matrix inversion and matrix determinant. Furthermore, a detailed analysis is included to show that the error between the demanded torque and the CMG output torque is inversely proportional to the square of the maximum achievable gimbal rate of the actuator. This allows drawing relationships between required precision and gimbal-rate capacity. The new steering law also breaks the symmetry in the computation of the gimbal rates, and thus the gimbal trajectories avoid the internal singularities, rather than passing through them. Consequently, the full CMG momentum space is used. For the derivation of the steering law, $\mathcal{H}_\infty$ theory is used, and an efficient adaptation algorithm is developed to account for the dependence of the Jacobian on the gimbal angles. Numerical results are included to demonstrate the singularity avoidance and escaping properties of the new FS law, leading to higher values than with the generalized singularity robust steering law for the CMG momentum.

Acknowledgments

The author would like to thank the reviewers and the Associate Editor for their insightful comments and suggestions.

References

[1] Margulies, G., and Aubrun, J. N., "Geometric Theory of Single-Gimbal Control Moment Gyro Systems," *Journal of the Astronautical Sciences*, Vol. 26, No. 2, 1978, pp. 159–191.

[2] Vadali, S. R., Walker, S. R., and Oh, H. S., "Preferred Gimbal Angles for Single Gimbal Control Moment Gyros," *Journal of Guidance, Control, and Dynamics*, Vol. 13, No. 6, 1990, pp. 1090–1095.

[3] Defendini, A., Faucheux, P., Guay, P., Morand, J., and Heimel, H., "A Compact CMG Product for Agile Satellites," *5th ESA International Conference on Spacecraft Guidance, Navigation and Control Systems*, edited by K. Fletcher and R. A. Harris, SP-516, ESA, Paris, 2003, pp. 27–32.

[4] Lappas, V. J., Steyn, W. H., and Underwood, C., "Design and Testing of a Control Moment Gyroscope Cluster for Small Satellites," *Journal of Spacecraft and Rockets*, Vol. 42, No. 4, 2005, pp. 729–739.

[5] Paradiso, J. A., "Global Steering of Single Gimballed Control Moment Gyroscopes Using a Directed Search," *Journal of Guidance, Control, and Dynamics*, Vol. 15, No. 5, 1992, pp. 1236–1244.

[6] Bedrossian, N. S., Paradiso, J., Bergmann, E. V., and Rowell, D., "Steering Law Design for Redundant Single-Gimbal Control Moment Gyroscopes," *Journal of Guidance, Control, and Dynamics*, Vol. 13, No. 6, 1990, pp. 1083–1089.

[7] Bedrossian, N. S., "Steering Law Design for Redundant Single Gimbal Control Moment Gyro Systems," M.S. Thesis, Massachusetts Inst. of Technology, Cambridge, MA, Aug. 1987.

[8] Wie, B., Bailey, D., and Heiberg, C., "Singularity Robust Steering Logic for Redundant Single-Gimbal Control Moment Gyros," *Journal of Guidance, Control, and Dynamics*, Vol. 24, No. 5, 2001, pp. 865–

872.

[9] Oh, H. S., and Vadali, S. R., "Feedback Control and Steering Laws for Spacecraft Using Single Gimbal Control Moment Gyros," *Journal of the Astronautical Sciences*, Vol. 39, No. 2, 1991, pp. 183–203.

[10] Wie, B., "Singularity Escape/Avoidance Steering Logic for Control Moment Gyro Systems," *Journal of Guidance, Control, and Dynamics*, Vol. 28, No. 5, 2005, pp. 948–956.

[11] Ford, K. A., and Hall, C. D., "Singular Direction Avoidance Steering for Control-Moment Gyros," *Journal of Guidance, Control, and Dynamics*, Vol. 23, No. 4, 2000, pp. 648–656.

[12] Avanzini, G., "Gimbal-Position Command Generation for a Cluster of Control Moment Gyroscopes," *Astrodynamics 2005: Proceedings of the AAS/AIAA Astrodynamics Conference*, Univelt, San Diego, CA, 2005, p. 2669.

[13] Kuhns, M. D., and Rodriguez, A. A., "Singularity Avoidance Control Laws for a Multiple CMG Spacecraft Attitude Control System," *Proceedings of the 1994 American Control Conference*, American Automatic Control Council, Evanston, IL, 1994, pp. 2892–2893.

[14] Krishnan, S., and Vadali, S. R., "An Inverse-Free Technique for Attitude Control of Spacecraft Using CMGS," *Acta Astronautica*, Vol. 39, No. 6, 1996, pp. 431–438.

[15] Wie, B., "Singularity Analysis and Visualization for Single-Gimbal Control Moment Gyro Systems," *Journal of Guidance, Control, and Dynamics*, Vol. 27, No. 2, 2004, pp. 271–282.

[16] Doyle, J., Glover, K., Khargonekar, P., and Francis, B., "State-Space Solutions to Standard $\mathcal{H}_2$ and $\mathcal{H}_\infty$ Control Problems," *IEEE Transactions on Automatic Control*, Vol. 34, No. 8, 1989, pp. 831–847.